OG.1.1.21

The Flux of Cosmic Ray Antiprotons from 3.7 to 24 GeV

G. Basini[1], R. Bellotti[5], M.T. Brunetti[3], F. Cafagna[5], M. Circella[5], A. Codino[3], C. De Marzo[5], M.P. De Pascale[4], R. L. Golden[6,*], C. Grimani[3], M. Hof[7], M. Menichelli[3], W. Menn[7], J.W. Mitchell[8], A. Morselli[4], J.F. Ormes[8], P. Papini[2], C. Pfeifer[7], S. Piccardi[2], P. Picozza[4], M. Ricci[1], M. Simon[7], P. Spillantini[2], S. A. Stephens[9], S.J. Stochaj[6] and R.E. Streitmatter[8]

[1]*Laboratori Nazionali INFN, I-00044 Frascati, Italy*

[2]*Dipartimento di Fisica dell'Università, and Sezione INFN di Firenze, I-50125 Firenze, Italy*

[3]*Dipartimento di Fisica dell'Università and Sezione INFN di Perugia, I-06100 Perugia, Italy*

[4]*Dipartimento di Fisica dell'Università and Sezione INFN di Roma, Tor Vergata, I-00133 Roma, Italy*

[5]*Dipartimento di Fisica dell'Università and Sezione INFN di Bari, I-70126 Bari, Italy*

[6]*New Mexico State University, Las Cruces, NM 88003, USA*

[7]*Universität Siegen, 57068 Siegen, Germany*

[8]*NASA/Goddard Space Flight Center, Greenbelt, MD 20771, USA*

[9]*Tata Institute of Fundamental Research, Bombay 400 005, India*

[*]*Deceased*

Abstract

The Matter Antimatter Superconducting Spectrometer, NMSU-WIZARD/MASS91 was flown from Fort Sumner, New Mexico on 23 September 1991. Using a magnetic spectrometer, time-of-flight counter, imaging calorimeter and a gas Cherenkov counter, the antiproton flux was measured between energies of 3.7 and 24.1 GeV for the first time. We found the flux value to be consistent with theoretical predictions for secondary production.

1 Introduction

The study of antiprotons has been an elusive goal of cosmic ray research for more than 20 years. The small flux of antiprotons compared to the large number of background particles makes antiproton measurements a great challenge to experimenters. Early experiments (Golden et al. 1984, Buffington et al. 1981) concentrated on the detection of antiprotons and reported their results as the ratio of the number of antiprotons to the number of protons measured. Ratio measurements do not require a detailed knowledge of the efficiencies for the various detector subsystems and are therefore much easier measurements to perform. Theoretical models of antiproton production predict fluxes and hence are not directly comparable to ratio measurements without first making some assumptions about the absolute proton flux and the efficiency of the detectors. The detectors of the MASS91 experiment were designed to combine the necessary rejection power to identify antiprotons, with the ability to evaluate the in-flight efficiencies needed for flux measurements. The measured flux of antiprotons can be directly compared to theoretical values to reveal properties of cosmic ray propagation. Excesses in the measured flux over the predicted value, or structure in the spectrum may hint at additional sources of antiprotons including the decay of dark matter particles.

2 The MASS91 Instrument

A schematic of the MASS91 instrument is shown in Figure 1. The detector components include a magnetic spectrometer, a plastic scintillator time-of-flight (ToF) system, a gas Cherenkov counter and an imaging calorimeter. A measurement of the particle's momentum and the sign of each particle's charge were derived from measurements made with the spectrometer. The magnitude of the charge and the direction the particle traversed the instrument was determined by the ToF system. Lighter, charge one particles were distinguished from anti(protons) by the Cherenkov counter. This detector had a Lorentz threshold of γ_{th}=25.5, which for (anti)protons corresponds to a kinetic energy of 24 GeV. Below this energy, particles lighter than protons produced a saturated Cherenkov light level while (anti)protons produced no Cherenkov signal.

The spectrometer consisted of a single coil superconducting magnet and a dual tracking system using drift chambers (Hof et al., 1994) and multiwire proportional chambers (MWPC) (Golden et al., 1991). Together, the tracking systems provided 19 position measurements in the bending direction and 11 position measurements in the non-bending direction. The deflection ($\eta = 1/R$) was determined using an iterative χ^2 process. This system provides a maximum detectable rigidity of 210 GV/c.

The ToF system consisted of two planes separated by 236 cm. The top ToF plane was composed of two scintillators stacked on top of one another. This configuration provided three independent dE/dx measurements and had a timing resolution of 370 ps for singly charged particles.

The gas Cherenkov counter was used as a threshold device to reject light particles (mainly muons) for the identification of antiprotons. The Cherenkov counter was located at the top of the payload. After passing through 1 m of the radiator gas (Freon 12), the Cherenkov light produced along that path was focused by a 4 segment mirror onto 4 phototubes . Each segment was a pie-shaped section of a spherical mirror (1.5 mm Polystyrene, aluminized) with a radius of 40 inches.

The imaging calorimeter consisted of 40 layers of 8 mm wide brass streamer tubes. Each of these layers had 64 tubes and alternate layers were arranged perpendicular to one another to provide both x and y projections. The walls of the tubes served as the passive converting material providing, 7.33 radiation lengths for the electromagnetic cascade development and an interaction mean free path of 0.75 for protons.

The instrument was launched on September 23, 1991 from Fort Sumner, New Mexico, where the geomagnetic cut off rigidity is approximately 4.5 GV/c. The payload took data for 9.8 hours at a float altitude with a mean residual atmosphere of 5.8 g/cm^2.

3 Flight Data Analysis

Antiprotons are a very rare component of the cosmic radiation. In order to accurately measure this species, great care must be taken to clearly identify antiprotons and effectively reject background events. Background events include: upward moving albedo protons, spillover protons (protons whose rigidity is mistakenly identified as negative) and light charge one particles (electrons, muons, pions and kaons). The ToF-system with its timing resolution of 370 ps separates albedo particles by more than 30 sigma. Therefore the albedo proton background can be neglected. The following strict cuts on the tracking system were used to protect against spillover protons and assure an accurate momentum determination: i) The number of planes used in the fit must be at least 15 out of 19 in the bending direction and 8 out of 11 in the nonbending direction. ii) The normalized χ^2 in each view must be less than 4. iii) The error in the measured deflection should be less than 0.02 c/GV. iv) The deflection determined using only the top half of the tracking system must agree with the deflection determined using only the bottom half of the tracking system to within 4 standard deviations. This cut eliminated hard-scatter events.

The gas Cherenkov counter was used to reject the remaining class of background events, the light particles. This component is dominated by atmospherically produced muons. Ex-

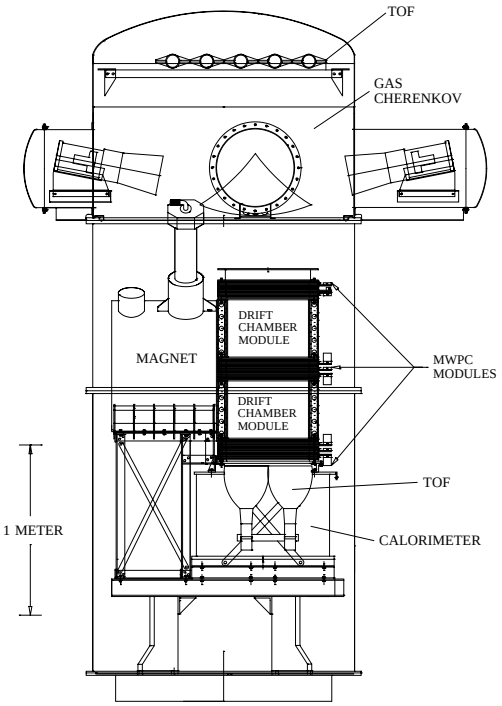

Figure 1: Schematic diagram of the NMSU-WIZARD/MASS91 apparatus.

tensive Monte Carlo studies, along with ground measurements, were performed in order to understand the behaviour of the Cherenkov detector. The light collection efficiency of the mirror is position dependent. Along the seams of the mirror segments and in the center of the mirror the light collecting power is reduced. These parts of the mirror were excluded from the analysis. For the remaining portions of the mirror, we observed an average number of 18.4 photoelectrons. We called the Cherenkov counter OFF when the signal from the part of the mirror hit by the Cherenkov light was less than 10% that of a saturated particle. This results in a muon rejection inefficiency of less than 0.2% within the rigidity region of this analysis.
No cuts were made on the data from the calorimeter. There was only a geometrical cut that required the track of the particle to pass through the sensitive volume of the calorimeter. This cut was implemented so that the imaging capabilities of the calorimeter could be used to check for biases and help determine the efficiencies.

4 Results

Applying all the selection criteria described above, including the Cherenkov OFF cut, all particles, within the rejecting efficiency of the Cherenkov counter, with velocities greater than the Cherenkov threshold are suppressed. The remaining events have the deflection distribution shown in Figure 2. The ordinate for negative deflection particles is blown up by a factor of 100. On the right hand side the high rigidity (low deflection) protons are suppressed. The solid line to the left is from a simulation of the Cherenkov counter's inefficiency to reject muons and pions. The solid line to the right is from a simulation of the Cherenkov inefficiency for protons and includes the spectrometer resolution function.

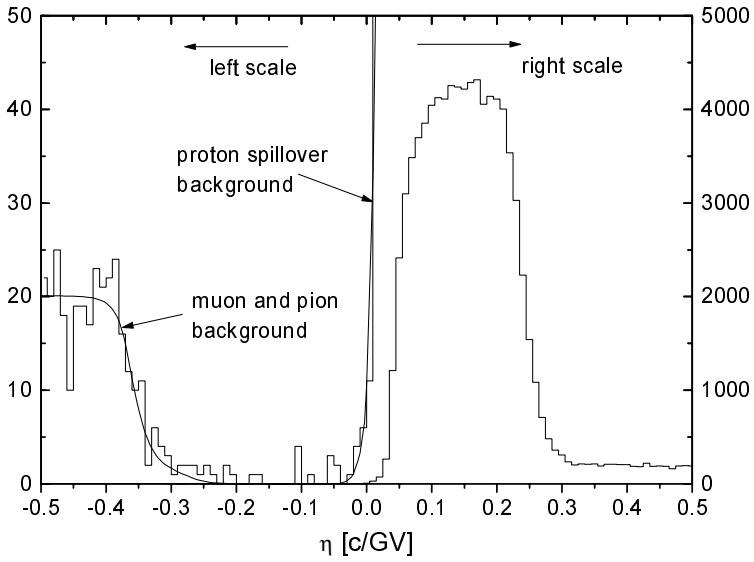

Figure 2: Data from the flight using all the selection criteria described in the text, including the Cherenkov OFF cut. All events detected with Cherenkov light are rejected.

The events in the region where these two lines are close to zero were identified as antiproton candidates. This region was divided into three intervals. The first interval extended from a deflection of -0.22 c/GV, which is close to the geomagnetic cutoff, to -0.14 c/GV. The second interval extends up to -0.08 c/GV, which is about the Cherenkov threshold for kaons. The third interval extends up to the Cherenkov threshold for antiprotons, -0.04 c/GV. In each of these intervals, 5 antiproton candidates were identified.
Due to the small but finite inefficiency of the Cherenkov counter for rejecting muons, it was necessary to subtract a muon background from each of the bins. This correction was 0.5 events in the low rigidity interval, 0.06 in the medium interval and 0.01 for the highest rigidity region. We assume that by using our strict selection criteria all interactions which occur above the bottom scintillator were rejected. Therefore, a correction had to be made for $\overline{p}'s$ that interacted in the instrument material (4.443 g/cm^2) above the bottom ToF. The correction factors were found to be 1.076, 1.070 and 1.066 for the low, medium and high rigidity intervals respectively. In order to get the total number of antiprotons entering at the top of the instrument, $N_{\overline{p}}^{TOI}$,the efficiencies of the particle selection criteria must be taken into account. Great care was used in the evaluation of these numbers: $\varepsilon_{trigger}$=(83$\pm$1)%, $\varepsilon_{scintillator}$=(97.3$\pm$1)%, $\varepsilon_{tracking}$=(82.8$\pm$2)% and $\varepsilon_{telemetry}$=98.2% .
Using these corrections and efficiencies, the total number of antiprotons, $N_{\overline{p}}^{TOI}$ entering at the top of the instrument (TOI), was calculated. We obtained 7.4 $\overline{p}$'s for the low energy interval from 3.7 to 6.3 GeV, 8.1 $\overline{p}$'s for the medium interval from 6.3 to 11.6 GeV and 8.1 $\overline{p}$'s for the high energy interval from 11.6 to 24.1 GeV.

These counts were converted to antiproton fluxes (TOI) by including the geometry factor, (123.3$\pm$1)cm^{2}sr, and livetime, (22345$\pm$70)s, of the instrument. Three additional corrections were implemented to extrapolate the TOI flux values to the top of the atmosphere (TOA). First, the number of antiprotons produced in the 5.8 g/cm^2 of atmosphere above the experiment was determined using the calculations done by Stephens (1993) and Pfeifer, Roesler, and Simon (1996). The number of atmospheric antiprotons was determined for each of the three energy bins and subtracted from the TOI numbers. Second, a correction factor for the antiprotons lost through interactions in the atmosphere was determined for each bin. The multiplicative correction factors are 1.102, 1.095 and 1.088 for the three bins respectively.

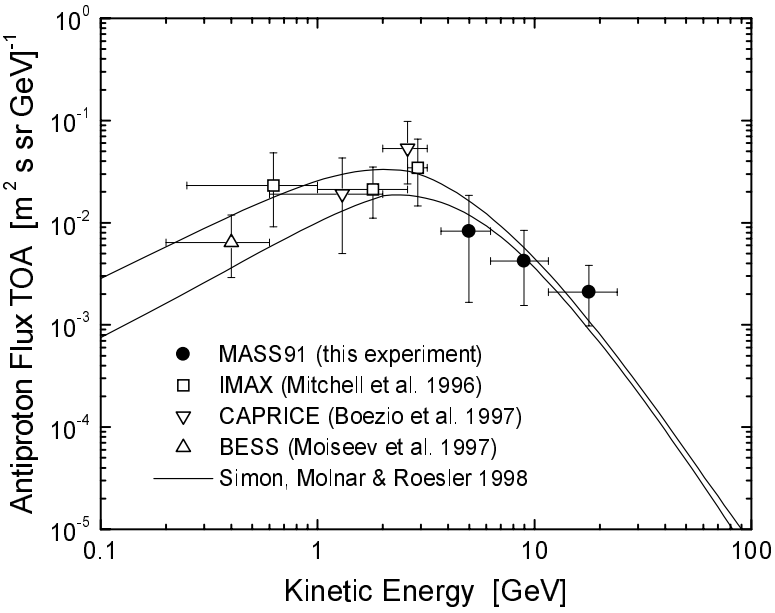

Figure 3: Measured antiproton flux of the NMSU-WIZARD/MASS91 experiment in comparison with other data and the error bands of a calculation by Simon, Molnar & Roesler, 1998.

The third term accounted for the transmission factor through the Earth's magnetic field. This term was derived using the helium events measured with the instrument. A power law interstellar helium spectrum was fit to the measured data above 20 GV/c. This spectrum was then solar modulated and compared to the measured helium spectrum at lower rigidities. The transmission function was found to be 85%, 98%, and 100%, for the three intervals respectively. An error of $\pm$3.5% was assumed for the lowest rigidity bin due to the uncertainty in the modulation parameter.

Combining these corrections yields the following flux values at the top of the atmosphere: $8.2^{+10.3}_{-6.6}$ for the 3.7 to 6.3 GeV bin, $4.2^{+4.2}_{-2.7}$ for the 6.3 to 11.6 GeV bin and $2.1^{+1.7}_{-1.1}$ for the 11.6 to 24.1 GeV bin, all in units of 10^{-3} [m^2 s sr GeV]. Figure 3 shows these measurements along with all other existing $\overline{p}$-flux measurements. The measurements are consistent, within the uncertainties, with the predictions of standard leaky box models in which $\overline{p}$-flux is purely secondary in nature.

References

Boezio, M., et al. 1997, ApJ , 487, 415
Buffington, A., et al. 1981, ApJ , 248, 1179
Golden, R.L., et al. 1984, ApJ, 287, 622
Golden, R.L., et al. 1991, Nucl. Instr. Meth., A306, 366
Hof, M. et al. 1994, Nucl. Instr. Meth., A345, 561
Mitchell, J.W., et al. 1996, Phys. Rev. Lett. , 76, 3057
Moiseev, A., et al. 1997, ApJ , 474, 479
Pfeifer, C., Roesler, S. & Simon, M., 1996, Phys. Rev. C , 54, 2
Simon, M., Molnar, A. & Roesler, S., 1998, ApJ , 499, 250
Stephens, S.A., Proc. 23rd ICRC (Calgary, 1993), 2, 144